Available online at www.sciencedirect.com

ScienceDirect

Procedia CIRP 65 (2017) 248 – 252

www.elsevier.com/locate/procedia

3rd CIRP Conference on BioManufacturing

Impact of hard machining on zirconia based ceramics for dental applications

Berend Denkena[a], Bernd Breidenstein[a], Sarah Busemann[a,*], Claudius Moritz Lehr[b]

[a]*Institute of Production Engineering and Machine Tools (IFW), Leibniz Universität Hannover, An der Universität 2, 30823 Garbsen, Germany*
[b]*Department of Prosthetic and Biomedical Materials Science, Hannover Medical School, Carl-Neuberg-Str. 1, 30625 Hannover, Germany*

* Corresponding author. Tel.: +49-511-762-18279; fax: +49-511-762-5115. *E-mail address:* busemann@ifw.uni-hannover.de

Abstract

Since the late 90s the use of zirconia based all-ceramic restorations increases. Many manufacturing steps are necessary, like pre-sintering, soft machining (pre-sintered condition), sintering and hard machining (fully sintered) in combination with a final staining or veneering step. All these techniques, especially hard machining, are associated with the production of flaws in different scales, in conjunction with thermal and residual stresses and phase transformations. These are inter alia capable to induce failure.

This work investigates the impact of hard machining on the material properties and attempts to establish a correlation to failure.

Peer-review under responsibility of the scientific committee of the 3rd CIRP Conference on BioManufacturing 2017

Keywords: ceramic; zirconia, hard machining; surface and subsurface properties

1. Introduction

The use of zirconia based ceramics for dental applications increased since the late 90s because of their superior mechanical as well as aesthetic properties [1].

The techniques for manufacturing zirconia based all-ceramic dental restorations are in a continuous state of development, modern dentistry is not imaginable without computer-aided-design/computer-aided-manufacturing (CAD/CAM) any more [2]. Nevertheless, manual process steps are still necessary in the technical process chains. Most systems machine partially sintered blanks, this includes designing an enlarged geometry and milling it from a partially sintered zirconia blank. The geometry has a linear shrinkage of 20-25% during sintering until it reaches its final dimensions [3]. Due to the shrinkage, there are sintering distortions, the object has to be reprocessed and adapted, the fully sintered zirconia has to be finished by grinding. This so called hard machining results in complex influences on the near-surface material layers, it can have an effect in two different directions: On the one hand, surface near compressive residual stresses can be induced as a consequence of the plastic deformation and due to tetragonal to monoclinic phase transformation. These stresses can increase the flexural strength. The individual mechanisms are not sufficiently known yet, but many investigations show that mechanical as well as thermal loads form residual stresses [4, 5]. On the other hand, grinding can introduce surface flaws [6, 7]. These can act as stress concentrators and decrease strength, if they are larger than the thickness of the grinding induced compressive residual stress layer [8, 9]. For the machining of fully sintered zirconia considerable time is required. Economic aspects of the machining process as well as the resulting product quality play a decisive role for the application of zirconia. Therefore, an efficient grinding process which results in required material properties like roughness, plastic deformation, damage and residual stresses is necessary. The mechanical properties of zirconia are depending not at least on the ability of phase transformation. For example machining induced cracks up to a critical size can be stopped by transformation from the tetragonal to the monoclinic phase. This effect is based upon the increase of the unit cell size during phase transformation, which induces compressive residual stresses and thus hinders the cracks from propagation [1, 6, 10, 11]. Phase transformation is influenced by the material removal mechanism, which can be more ductile or brittle [12, 13]. A scale for this is the critical uncut chip thickness $h_{cu,crit}$. The aim of this work is to determine

Peer-review under responsibility of the scientific committee of the 3rd CIRP Conference on BioManufacturing 2017
doi:10.1016/j.procir.2017.04.055

the influence of various grinding process parameters on the material properties roughness, residual stresses and phase transformation in grinding zirconia.

2. Experimental conditions

2.1. Experimental setup

For these investigations the grinding process was carried out as a standard face grinding process. The experiments are conducted on a 5-axis CNC machine tool (Röders RFM 600 DS). Cutting speed v_c, depth of cut a_e and abrasive grain size d_g are varied, the feed rate f is constant. The parameters are summarized in Table 1. A wet grinding process is applied, as coolant a 5% oil-in-water emulsion is used. The specimens are fixed with dental sticky wax onto a workpiece carrier (see Figure 1). Before the main experiments can be performed, as preparatory work the specimens have to be face ground onto the same level. This is necessary to generate comparable results without an effect of the manual manufacturing of specimens.

Table 1. Parameters – face grinding

Process parameter	
Cutting speed	v_c = 10, 30 m/s
Depth of cut	a_e = 0.005, 0.1 mm
Feed rate	v_f = 800 mm/min
Specific material removal rate	Q'_w = 0.07; 1.33 mm³/s·mm

The grinding tool topography is measured by means of an SEM. After grinding surface roughness, monoclinic phase content and resulting residual stresses are measured. Surface roughness of the ground specimens is measured in a tactile way by a stylus instrument (Perthometer Concept) with the parameters given in Table 2.

Table 2. Parameters for roughness measurement.

Parameter	D15, D251
Cut off length	λ_c = 0.8; 2.5 mm
Traversing length	l_{tl} = 4; 7.5 mm

Residual stresses are measured applying the sin²ψ–method using a GE XRD 3003 ETA diffractometer with a 2 mm collimator and Co Kα–radiation with 30 kV and 40 mA with a maximum penetration depth of τ = 3.1 µm. Residual stresses are measured parallel and transverse to the grinding direction. The quantity of the monoclinic phase is measured in the surface near region to a maximum depth of 1.5 µm.

2.2. Grinding tools

For this investigation grinding wheels with 1A1-geometry and natural diamond as abrasive grain with an average grain size of d_g = 15 µm and d_g = 251 µm (Figure 1) and electroplated bonding are used. The tool properties are summarized in Table 3. Usually resin bond grinding tools are used for grinding zirconia components due to their higher flexibility and porosity. But for small components like dental crowns and bridges, it is technically unconvertible, so state of the art in dental manufacturing are electroplated grinding tools [2].

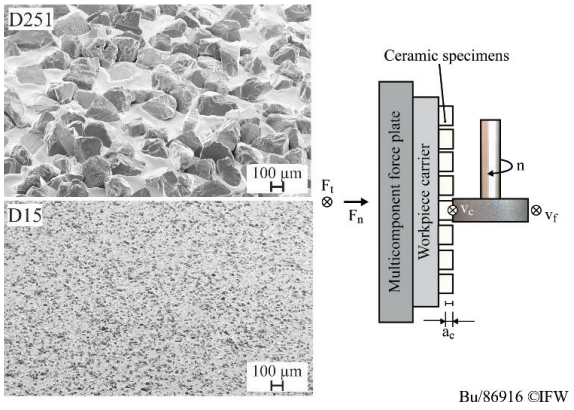

Figure 1. Tool topography and experimental setup.

Table 3. Tool properties.

Diameter	40 mm
Geometry	1A1, cylindrical
Abrasive	natural diamond
Grain size	D15, D251
Bonding	electroplated

2.3. Material

The material used in this investigation is a commercially available zirconia based dental ceramic. The tetragonal phase is doped with 4.5 - 6 wt.% yttrium oxide (Y_2O_3). The mechanical properties at room temperature for the dense material are shown in Table 4.

Table 4. ZrO_2 properties

Mechanical properties		
Density	g/cm³	> 6.04
Flexural strength	MPa	1.500
Compressive strength	MPa	3.000
Young's modulus E	MPa	205.000
Fracture toughness K_{IC}	MPa $m^{0.5}$	8
Hardness H	HV 0.5	1.300

The material comes as a pre-sintered blank. The needed specimens are separated in an enlarged geometry by a precision table saw and then sintered densely. The specimens are heated up to a desired temperature of 1450 °C with a rate of 8 °C/min. The desired temperature is hold for 2:00 h and then cooled down to room temperature with a cooling rate of 8 °C/min. The parameters are summarized in Table 5. The ready-for-use specimens have a size of 30 mm x 15 mm x 1.5 mm. The microstructure of the dense material has an average grain size of 0.4 µm.

Table 5. Sintering conditions.

step	initial temperature [°C]	desired temperature [°C]	heating/ cooling rate [°C/min]	holding time [h:min]
1	20	1450	8	3:00
2	1450	1450	0	2:00
3	1450	20	8	3:00

3. Experimental results and discussion

The uncut chip thickness is varied by changing grain size, grinding speed and depth of cut in order to study the material removal mechanisms when grinding zirconia and its influence on roughness, residual stresses and phase transformation. The critical uncut chip thickness $h_{cu,crit}$ depending on the material properties, has a calculated value of 0.895 µm, according to (1) [12, 14] with $\Psi = 0.15$ [12] and the material properties given in Table 1:

$$h_{cu,crit} = \psi \cdot \left(\frac{E}{H}\right) \cdot \left(\frac{K_{IC}}{H}\right)^2 \quad (1)$$

The uncut chip thickness h_{cu} is calculated according to [15]:

$$h_{cu} = \frac{1}{\sqrt{3}} \left(\frac{v_f}{v_c} \cdot \frac{3}{\lambda \cdot N_{GV}} \cdot \frac{a_e}{l_g} \right)^{\frac{1}{3}} \quad (2)$$

The parameters λ (form factor of grain) and N_{GV} (amount of grains per cm³) are measured based on the surface topography of the grinding wheel before the first tests (Figure 1). The form factor of grain is defined as shown in (3), the value for κ_G (cutting edge aperture angle) is assumed with 150 °.

$$\lambda = \tan\left(\frac{\kappa_G}{2}\right) \quad (3)$$

For the amount of grains per cm³ (N_{GV}), the grains in the top view of a SEM picture are counted for a an area of a square centimetre and then extrapolated over the grain size to the volume. For the tool with a grain size of 15 µm, N_{GV} has an amount of 10133333/ cm³, for the tool with a grain size of 251 µm, N_{GV} has an amount of 47809/ cm³.
The wear caused by the grinding process is not taken into account although the grinding tool conditions change during the process. So the calculated uncut chip thickness shows the initial values and a trend for the absolute ones.

In Figure 2 and Figure 3 SEM pictures of ground surfaces are shown. The calculated chip thickness for the surface in Figure 3 is 0.42 µm, thus it is smaller than the calculated critical uncut chip thickness of 0.895 µm. The result is an even surface with evenly distributed grinding marks, the ceramic is removed in a more ductile mode. In Figure 2 the calculated uncut chip thickness is 2.52 µm, so it is higher than the calculated critical

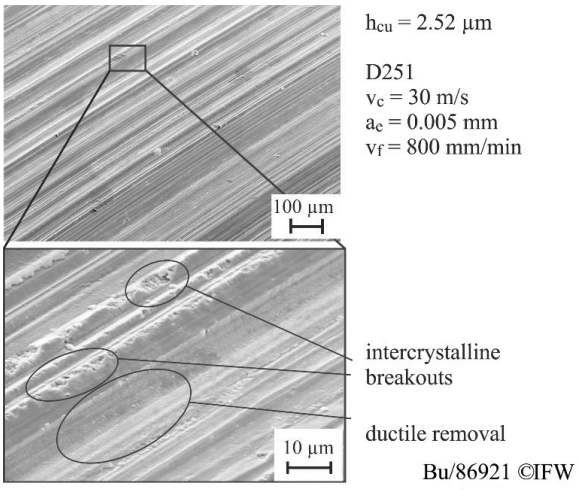

Figure 2. Surface topography of ground surface with h_{cu} = 2.52 µm.

uncut chip thickness. The surface shows brittle intercrystalline breakouts, high roughness and bulging at the scratch edges. The roughness increases with uncut chip thickness. Nevertheless, also this surface shows areas, where the material is removed in a more ductile way. The grinding direction can be seen in both figures. The surfaces consist mostly of a series of parallel grinding marks, the width of these marks increases with increasing abrasive grain size. In both figures, the specific material removal rate Q'_w has a value of 0.07 mm³/s·mm. This shows that at a same productivity level the surface topography can differ in a wide range.

-

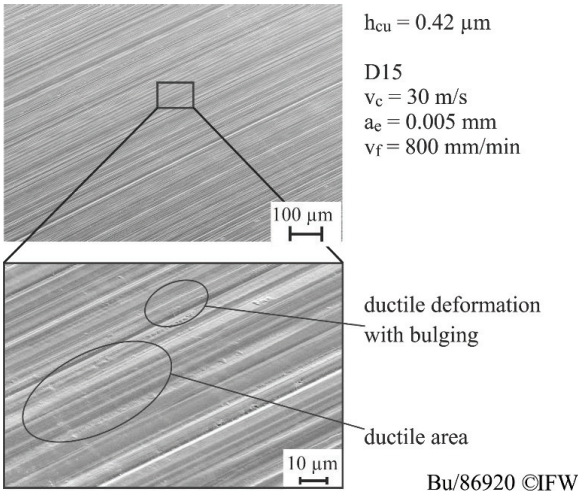

Figure 3. Surface topography of ground surface with h_{cu} = 0.42 µm.

In Figure 4 and Figure 5 the average surface roughness R_z, the maximum surface roughness R_{max} and the peak height R_p are depicted. The roughness is measured transverse to the grinding direction. Figure 4 shows the values for d_g = 15 µm and the maximum value is about 3 µm for an uncut chip thickness of 1 µm. When the uncut chip thickness is higher than 0.7 µm roughness increases.

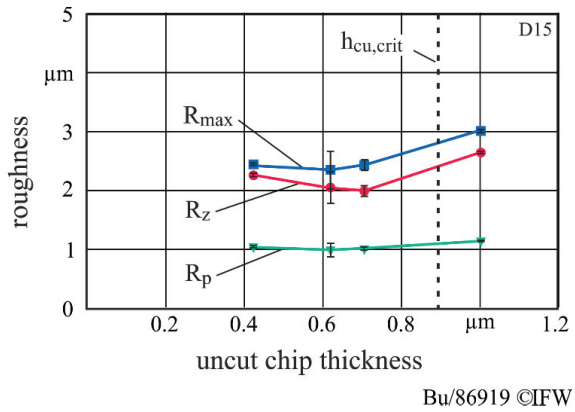

Figure 4. Roughness depending on uncut chip thickness, d_g = 15 µm

Figure 5 shows the values for d_g = 251 µm and the maximum value is about 34.5 µm for an uncut chip thickness of 2.4 µm. The overall surface roughness is 10 times higher than the surfaces ground with d_g = 15 µm. If the graphs of R_z and R_{max} are compared a trend can be suspected: When the graphs for the maximum and average roughness have a similar development (Figure 4) the generated surfaces are even as well (Figure 3). When the graph development is uneven (Figure 5) it indicates a surface with breakouts and an uneven distribution of the grinding marks (Figure 2).

In both figures, R_p stays almost constant. The ratio R_p / R_z is an indicator for the surface profile shape. A value smaller than 0.5 describes a round surface profile shape and a value higher than 0.5 a sharp one [16]. For Figure 4 and Figure 5 the R_p / R_z ratio has a range from 0.46 to 0.52, so there is no significant difference.

In Figure 6 the measured values of the residual stresses corresponding to the calculated uncut chip thickness are shown. The residual stresses for the as-fired specimens in both directions (transverse and parallel) have a value of -3 to -9 MPa, so they are, in consideration of the measurement error, “stress-free”. All near-surface measured stresses are compressive residual stresses. Up to a chip thickness of 1 µm the residual stresses show a slight decreasing trend. With further increasing uncut chip thickness the residual stresses are increasing as well, this is in agreement with [4], showing

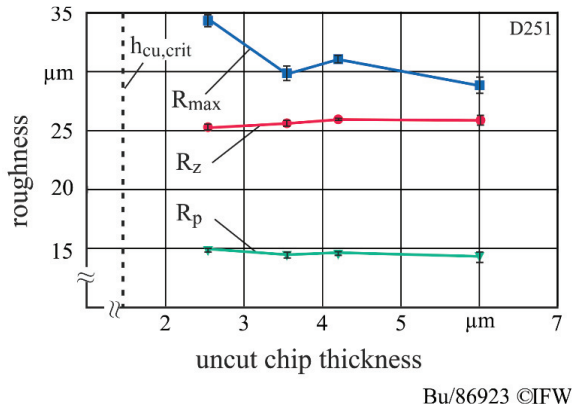

Figure 5. Roughness depending on uncut chip thickness, dg = 251 µm

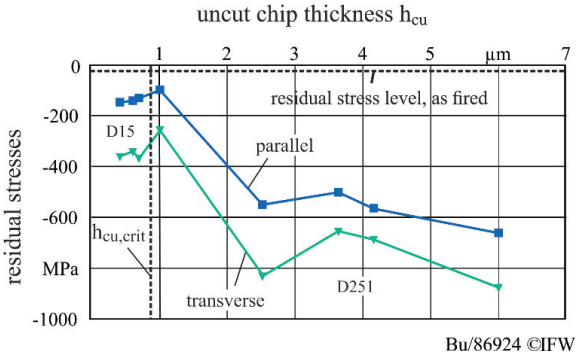

Figure 6. Residual stresses versus calculated uncut chip thickness

increasing compressive residual stresses with increasing uncut chip thickness. Compressive residual stresses in subsurface area are increasing with increasing surface roughness, this is coupled with increasing amounts of plastic deformation. The stresses transverse to grinding direction are up to 200 MPa stronger than the stresses parallel to grinding direction. As a reason for this strong plastic material deformation due to lateral displacement by the cutting abrasive grain size is assumed. It should be considered that the surface roughness for the specimens with high compressive residual stresses is higher than the penetration depth of the diffraction radiation, so only subsurface stresses are measured, the stresses at the grinding marks’ ground are not taken into account.

In Figure 7 the results for the residual stresses and the monoclinic phase depending on the calculated uncut chip thickness for d_g = 15 µm are shown. The amount of monoclinic phase was calculated by the levels of intensity according to [17]:

$$x_m = \frac{I_m(111) + I_m\left(1\,1\,\bar{1}\right)}{I_m(111) + I_m\left(1\,1\,\bar{1}\right) + I_t(111)} \tag{4}$$

I is for the integral intensity at 2θ, *t* is for the tetragonal peak and *m* for the main peak of the monoclinic phase. The amount of monoclinic phase shows a small increase up to an uncut chip thickness of 0.7 µm with decreasing residual stress. For an uncut chip thickness of 1 µm the amount decreases, but the values are in a range from 3.1 to 5.2 %, so considering the measured values referring to the measurement error, there is almost no difference.

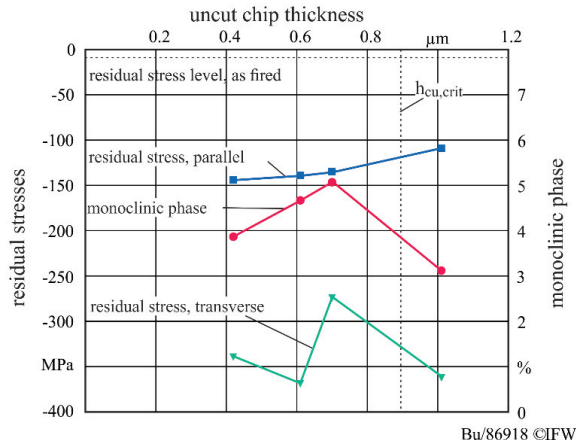

Figure 7. Residual stresses and monoclinic phase content for dg = 15 µm.

4. Conclusion and outlook

This paper shows, that varying the uncut chip thickness plays an essential role in hard machining zirconia based ceramics. The surface properties like e. g. residual stresses and roughness are depending on the process- and tool-properties, as well as the given material properties themselves. The abrasive grain size has a leading impact on the surface layer properties. For the analyzed material, compressive residual stresses are obtained with calculated uncut chip thicknesses up to 6 µm. Due to the high surface roughness it was not possible to define the amount of the monoclinic phase for the rough surfaces (h_{cu} > 1 µm) reliably, this has to be revised with other parameters. With uncut chip thickness up to 1 µm, however, there are amounts of monoclinic phase up to 5 %. This is absolutely within ISO 13356, which demands an amount below 20 % [18].

For future work it is necessary to find a possibility to measure the monoclinic phase content for very rough surfaces. Besides, it would be instructive to test the flexural strength as an indicator for inner damage and whether the defects are introduced by hard machining (e. g. cracks) or sintering (e. g. powder agglomerates, pores).

Acknowledgements

The authors would like to thank the German Research Foundation (DFG) for its support of the project “Investigation of bonding mechanisms between scaffolding and veneering materials”.

References

[1] Chevalier J, Gremillard L, Virkar AV, Clarke DR. The tetragonal - monoclinic transformation in zirconia: lessons learned and future trends. Journal of the American Ceramic Society 2009;92(9):1901-20.
[2] Luthardt RG, Holzhüter MS, Rudolph H, Herold V, Walter MH. CAD/CAM-machining effects on Y-TZP zirconia. Dental Materials 2004;20(7):655–62.
[3] Denry I, Kelly JR. State of the art of zirconia for dental applications. Dental Materials 2008;24(3):299–307.
[4] Lierse T. Mechanische und thermische Wirkungen beim Schleifen keramischer Werkstoffe. VDI-Verl., Düsseldorf, 1998.
[5] Hessert R, Eigenmann B, Vöhringer O, Löhe D. Fracture mechanical evaluation of the effects of grinding residual stresses on bending strength of ceramics. Materials Science and Engineering: A 1997;234-236:1126–9.
[6] Samuel R, Chandrasekar S, Farris TN, Licht RH. Effect of residual stresses on the fracture of ground ceramics. Journal of the American Ceramic Society 1989;72(10):1960–6.
[7] Zhang B, Zheng XL, Tokura H, Yoshikawa M. Grinding induced damage in ceramics. Journal of materials processing technology 2003;132(1):353–64.
[8] Kosmač T, Oblak C, Jevnikar P, Funduk N, Marion L. The effect of surface grinding and sandblasting on flexural strength and reliability of Y-TZP zirconia ceramic. Dental Materials 1999;15(6):426–33.
[9] Denry IL, Holloway JA. Microstructural and crystallographic surface changes after grinding zirconia - based dental ceramics. Journal of Biomedical Materials Research Part B: Applied Biomaterials 2006;76(2):440–8.
[10] Chevalier J. What future for zirconia as a biomaterial? Biomaterials 2006;27(4):535–43.
[11] Claussen N. Stress - Induced Transformation of Tetragonal ZrO2 Particles in Ceramic Matrices. Journal of the American Ceramic Society 1978;61(1-2):85–6.
[12] Bifano TG, Dow TA, Scattergood RO. Ductile-regime grinding: a new technology for machining brittle materials. Journal of engineering for industry 1991; 113(2):184–9
[13] Marinescu ID. Handbook of advanced ceramics machining. CRC Press; 2006.
[14] Jochum N. Zerspanung ultraharter Keramik am Beispiel einer dreigliedrigen Zahnbrücke, Diss., Eidgenössische Technische Hochschule ETH Zürich, Nr. 20833, 2013.
[15] Lierse T. Mechanische und thermische Wirkungen beim Schleifen keramischer Werkstoffe, Diss. , Leibniz Universität Hannover, 1998.
[16] Volk R. Rauheitsmessung: Theorie und Praxis. Beuth Verlag; 2013.
[17] Garvie RC, Nicholson PS. Phase analysis in zirconia systems. Journal of the American Ceramic Society 1972;55(6):303–5.
[18] DIN Deutsches Institut für Normung e. v.. Chirurgische Implantate-Keramische Werkstoffe aus yttriumstabilisiertem tetragonalem Zirkonoxid (Y-TZP) 11.040.40(DIN EN ISO 13356). Beuth Verlag; 2013.